Analysis of the Performance for SFBC-OFDM and FSTD-OFDM Schemes in LTE Systems over MIMO Fading Channels

Mohammad Torabi, Ali Jemmali, and Jean Conan
Department of Electrical Engineering,
École Polytechnique de Montréal,
Montréal, QC, Canada,
{mohammad.torabi, ali.jemmali, jean.conan}@polymtl.ca

***Abstract*— In this paper, a performance analysis is presented for space-frequency block coded orthogonal frequency division multiplexing (SFBC-OFDM) and Frequency Switched Transmit Diversity OFDM (FSTD-OFDM) schemes in the 3GPP Long Term Evolution (LTE) system over MIMO fading channels. Analytical expressions for the average BER, average channel capacity and the average throughput of the system are derived for two different MIMO schemes, SFBC-OFDM and FSTD-OFDM, defined in LTE, and are evaluated numerically. Monte-Carlo simulation results are also provided to verify the accuracy of the mathematical analysis. It is shown that the results obtained from Monte-Carlo simulations match closely with those obtained from the derived mathematical formulas.**

***Keywords*- Performance Analysis, MIMO, LTE, M-QAM Modulation, Capacity, Throughput.**

I. INTRODUCTION

To increase the capacity and speed of wireless communication systems, a new wireless data networks has been emerged and has been standardized by the 3rd Generation Partnership Project (3GPP). This new standard is a natural evolution to the existing second (2G) and third (3G) generation wireless networks in order to respond to the growing demand in terms of data rates and speed and marketed as 4G Long Term Evolution (LTE). In LTE, data throughput and the speed of wireless data are increased by using a combination of new methods and technologies like Orthogonal Frequency Division Multiplexing (OFDM) and Multiple-Input Multiple-Output (MIMO) techniques.

In the downlink, LTE transmission is based on Orthogonal Frequency Division Multiple Access (OFDMA), known as a technique for encoding digital data on multiple carrier frequencies. It was shown that OFDMA is an efficient technique to improve the spectral efficiency of wireless systems. By converting the wide-band frequency selective channel into a set of several flat fading subchannels, OFDM technique becomes more resistant to frequency selective fading than single carrier systems. As OFDM signals are in time and frequency domain, they allow adding frequency domain scheduling to time domain scheduling. In LTE, for a given transmission power, the system data throughput and the coverage area can be optimized by employing Adaptive Modulation and Coding (AMC) techniques. The role of a user scheduler at the transmitter side is to assign the data rate for each user according to the channel conditions from the serving cell, the interference level from other cells, and the noise level at the receiver side.

In LTE standard, the use of MIMO has been considered as an essential technique in order to achieve the target in terms of data throughput and reliability. MIMO is known to be a very powerful technique to improve the system performance of wireless communication systems. The diversity and multiplexing modes are the two main modes of operation of multiple antennas systems. The principle of diversity mode is based on transmitting the same signal over multiple antennas and hence to improve the reliability of the system by a diversity gain. In this mode, the mapping function of transmit symbols used at the transmit antennas is called Space Time Block Coding (STBC). On the other hand, multiplexing mode uses two or more different spatial streams and sends them through two different antennas, consequently, the data rate can be improved.

In [1] an analysis is performed for evaluating the average bit error rate (BER) of MIMO schemes in LTE systems employing the classical M-ary quadrature amplitude modulation (M-QAM) scheme. In this paper, we provide more details about the system model and about the considered transmit diversity schemes in LTE and we extend the results in [1] and in addition to the average BER analysis, we present the average capacity analysis as well as the average throughput analysis for two different MIMO schemes as defined in LTE. Then, the results obtained from analytical formulas are provided, showing the performance of the considered schemes. From those results one can simply compare the benefits of using considered MIMO schemes. In addition, the results obtained from Monte-Carlo simulations are also provided to verify the accuracy of the analysis for each performance metric.

To study the performance of LTE systems a MATLAB based downlink physical layer simulator for Link Level Simulation (LLS) has been developed in [2], [3]. A System Level Simulation of the Simulator is also available [4]. The goal of developing the LTE simulator was to facilitate comparison with the works of different research groups and it is publicly available for free under academic non-commercial use license [3]. The main features of the simulator are adaptive coding

and modulation, MIMO transmission and scheduling. As the simulator includes many physical layer features, it can be used for different applications in research [4]. In [5], the simulator was used to study the channel estimation of OFDM systems and the performance evaluation of a fast fading channel estimator was presented. In [6] and [7], a method for calculating the Precoding Matrix Indicator (PMI), the Rank Indicator (RI), and the Channel Quality Indicator (CQI) were studied and analyzed with the simulator.

In this paper, analyses of the performance for two transmit diversity schemes, known as Space Frequency Block Coding (SFBC) and Frequency Switched Transmit Diversity (FSTD) MIMO schemes in LTE system, are presented for different performance metrics. Those performance metrics are the average BER, the average capacity and the average throughput. The average BER results obtained from the analysis are then compared to the results of Monte-Carlo simulation using the Link Level LTE simulator [2], [3].

The remainder of this paper is organized as follows. In Section II, we present the system model used in the paper. In Section III, we present performance analyses for the average BER, the average capacity and the average throughput of SFBC and FSTD MIMO schemes. The numerical and simulation results and discussions are presented in Section IV. Finally, Section V concludes the paper.

II. System Model

In this section, the structure of the OFDM LTE signal and LTE transmit diversity schemes are described. However, more details can be found in [8]. The OFDM signal has a time and a frequency domains. In the time domain, the LTE signal is composed of successive frames. Each frame has a duration of $T_{\text{frame}} = 10$ *msec*. Each frame is divided into 10 subframes with equal length of 1 *msec*. Each subframe consists of two equal length time-slots with a time duration of $T_{\text{slot}} = 0.5$ *msec*. For a normal cyclic prefix length, each time-slot consists of $N_s = 7$ OFDM symbols. In the frequency domain, the OFDM technique converts the LTE wideband signal into several narrowband signals. Each narrowband signal is transmitted on one subcarrier frequency.

In LTE, the spacing between subcarriers is fixed to 15 KHz. Twelves adjacent subcarriers, occupying a total of 180 KHz, of one slot forms the so-called Resource Block (RB). The number of Resource Blocks in an LTE slot depends on the allowed system bandwidth. The minimum number of RB is equal to 6 corresponding to 1.4 MHz system bandwidth. For 20 MHz system bandwidth (Maximum Allowed bandwidth in LTE) the number of RB is equal to 100. In a MIMO system with M_R receive antennas and M_T transmit antennas, the relation between the received and the transmitted signals on subcarrier frequency k ($k \in 1, \cdots, K$), at sampling instant time n ($n \in 1, \cdots, N$) is given by

$$\mathbf{y}_{k,n} = \mathbf{H}_{k,n}\mathbf{x}_{k,n} + \mathbf{n}_{k,n} \tag{1}$$

where $\mathbf{y}_{k,n} \in C_{M_R \times 1}$ is the received vector, $\mathbf{H}_{k,n} \in C_{M_R \times M_T}$ represents the channel matrix on subcarrier k at instant time n, $\mathbf{x}_{k,n} \in C_{M_R \times 1}$ is the transmit symbol vector and $\mathbf{n}_{k,n} \sim \mathcal{CN}(0, \sigma_n^2.\mathbf{I})$ is a white, complex valued Gaussian noise vector with variance σ_n^2.

Assuming perfect channel estimation, the channel matrix and noise variance are considered to be known at the receiver. A linear equalizer filter given by a matrix $\mathbf{F}_{k,n} \in C_{M_R \times M_R}$ is applied on the received symbol vector $\mathbf{y}_{k,n}$ to determine the post-equalization symbol vector $\mathbf{r}_{k,n}$ as follows [7]

$$\mathbf{r}_{k,n} = \mathbf{F}_{k,n}\mathbf{y}_{k,n} = \mathbf{F}_{k,n}\mathbf{H}_{k,n}\mathbf{x}_{k,n} + \mathbf{F}_{k,n}\mathbf{n}_{k,n}. \tag{2}$$

The Zero Forcing (ZF) or Minimum Mean Square Error (MMSE) design criterion [9] are typically used for the linear receiver and the input signal vector is normalized to unit power. In MIMO-OFDM systems, the key factor of link error prediction and performances is the signal to noise ratio (SNR) which represents the measurement for the channel quality information. In this study, the SNR is defined by

$$\gamma_{k,n} = \frac{\overline{\gamma}}{N_T}\|\mathbf{H}_{k,n}\|_{\text{F}}^2 \tag{3}$$

where $\overline{\gamma} = E_s/N_0$ is the average SNR per symbol and $\|.\|_F^2$ is the squared Frobenius norm of a matrix.

A. LTE Frame Structure

Two types of LTE frame structures are defined depending on the duplexing mode of the transmission. Two duplexing methods are defined in LTE, namely Time Division Duplex (TDD) and Frequency Division Duplex (FDD). In the FDD mode, the downlink path (DL), from the eNodeB to user equipment (UE), and the uplink path (UL), from the UE to eNodeB, operate on different carrier frequencies. In the TDD mode, the downlink and the uplink paths operate on the same carrier frequency but in different time slots. In other word, in FDD, the downlink and uplink transmissions are separated in the frequency domain, whereas in TDD the downlink and uplink transmissions are separated in the time domain. Type 1 frame structure of LTE is associated with the FDD duplexing mode whereas Type 2 frame structure of LTE is associated with the TDD duplexing mode. For both types of LTE frame structures, the DL and UL transmissions in LTE systems are arranged into radio frames. The duration of a radio frame is fixed at 10 *msec*. The radio frame is comprised of ten 1 *msec* subframes, which represents the shortest Transmission Time Interval (TTI). Each subframe consists of two slots of duration 0.5 *msec*.

Frame structure of Type 1 LTE FDD and Type 2 TDD are shown in Figure 1(a) and Figure 1(b), respectively. In Type 2 TDD frame structure, as shown in Figure 1(b), each radio frame includes 2 half frames of 5 subframes each. Subframes can be either uplink subframes, downlink subframes or special subframes. Special subframes include the following fields: Downlink Pilot Time Slot (DwPTS) and Uplink Pilot Time Slot (UpPTS). Depending on the length of the Cyclic Prefix (CP) and the subcarriers spacing, each time slot consists of 6 or 7 OFDM symbols. In fact, the cyclic prefix represents

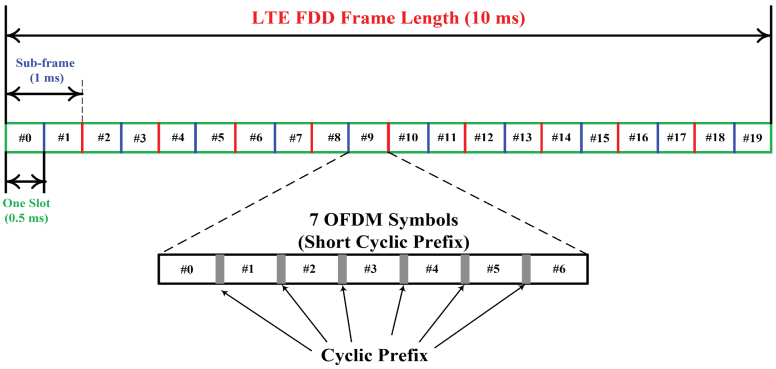

(a) Type 1 LTE FDD Frame Structure.

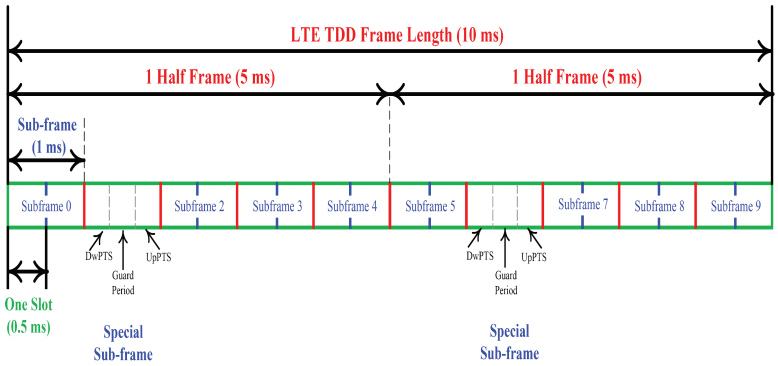

(b) Type 2 LTE TDD Frame Structure.

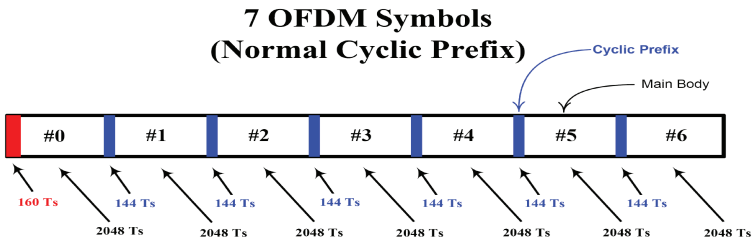

7 x 2048 Ts
+ 6 x 144 Ts
+ 1 x 160 Ts
15360 Ts = 0.5 ms

Ts=1/30720 ms

(c) Structure of the symbols in one slot with Normal Cyclic Prefix.

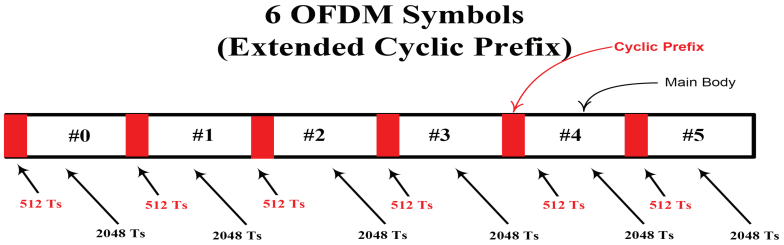

6 x 2048 Ts
+ 6 x 512 Ts
15360 Ts = 0.5 ms

Ts=1/30720 ms

(d) Structure of the symbols in one slot with Extended Cyclic Prefix.

Fig. 1. LTE Frame Structure.

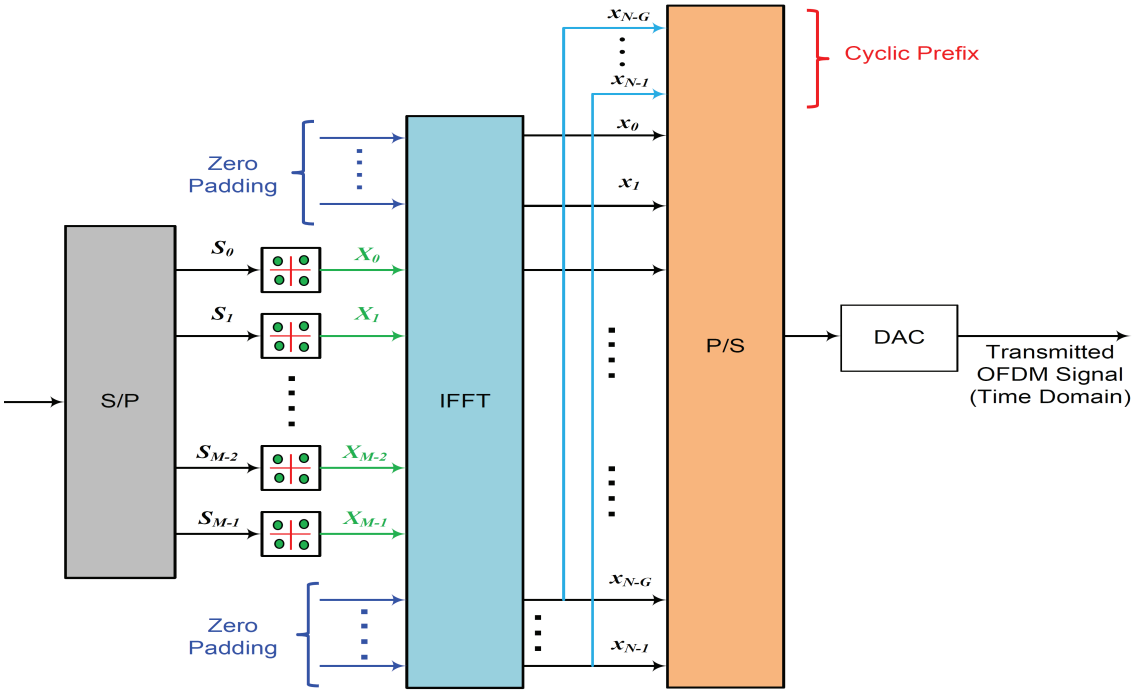

Fig. 2. OFDM Signal Generation.

a guard period at the beginning of each OFDM symbol which provides protection against multi-path delay spread. To effectively combat the delay spread of the channel, the duration of the cyclic prefix should be greater than the duration of the multi-path delay spread. At the same time, cyclic prefix also yields an overhead which should be minimized.

Two types of CP were specified in LTE, namely the normal CP and the extended CP. The structure of the symbols in a 0.5 *msec* time slot with *normal cyclic prefix* and *extended cyclic prefix* are shown in Figure 1(c) and Figure 1(d), respectively. As shown, in normal CP, each slot includes 7 OFDM symbols, whereas in extended CP each slot includes only 6 OFDM symbols. The duration of the first cyclic prefix and the subsequent prefixes in terms of sampling time (T_s) are also shown in Figure 1(c). T_s represents the basic time unit and is given by $T_s = 1/(15000 \times 2048)$ seconds. It can be noticed that the duration of the first cyclic prefix is larger than the subsequent cyclic prefixes. For the normal cyclic prefix the duration of the first cyclic prefix is defined as $160 \times T_s$, whereas the duration of subsequent cyclic prefixes is only $144 \times T_s$. For extended cyclic prefix, all prefixes have the same length of $512 \times T_s$. The normal cyclic prefix length is proposed to be sufficient for the majority of radio environment scenarios, while the extended cyclic prefix is intended for radio environment with particularly high delay spreads. As we will see later, the cyclic prefix of size G is the copy of G last elements from an OFDM block including N elements.

B. OFDM Symbol Generation

An OFDM symbol can be generated using the Inverse Fast Fourier Transform (IFFT), which is an operation of a transformation from frequency domain to time domain. Accordingly, the transmitted signal is defined in the frequency domain. This means that the complex modulated symbols are considered as the coefficients in the frequency domain. The block diagram of an OFDM signal generation is shown in Figure 2. The serial input data stream of size M are converted into M parallel data elements denoted a block given by $\mathbf{S} = (S_0, S_1, S_2, ..., S_{M-1})^T$. Then, M parallel data streams (S_i, $i = 0, 1, ..., M-1$) are independently modulated (e.g., M-QAM modulation) to form a vector of complex modulated symbols given by $\mathbf{X} = (X_0, X_1, X_2, ..., X_{M-1})^T$.

The vector $\mathbf{X}$ is then applied to the input of an N-point Inverse Fast Fourier Transform (IFFT). The output of this operation is a set of N complex time-domain samples, given by $\mathbf{x} = (x_0, x_1, x_2, ..., x_{N-1})^T$. In practical implementation of an OFDM system, N the size of IFFT is greater than M the number of modulated symbols (i.e., $N \geq M$).

As shown in Figure 2, for the remaining subcarriers ($N-M$ subcarriers) are being padded with zeros. The next important operation in the generation of an OFDM signal is the creation of a guard period at the beginning of each OFDM symbol by inserting a Cyclic Prefix (CP). This CP is simply generated by taking the last G samples of the IFFT output and appending them at the beginning of vector $\mathbf{x}$. This yields the OFDM symbol in the time domain, as a vector of size $G + N$, given by $(x_{N-G}, ..., x_{N-1}, x_0, x_1, x_2, ..., x_{N-1})^T$ as shown in Figure 2. The last step in the OFDM signal generation is the parallel to serial conversion of the IFFT output an then its transmissions through the transmit antennas. The generated OFDM signal will be transmitted over multiple transmit antennas using the transmit diversity schemes to be explained in the following.

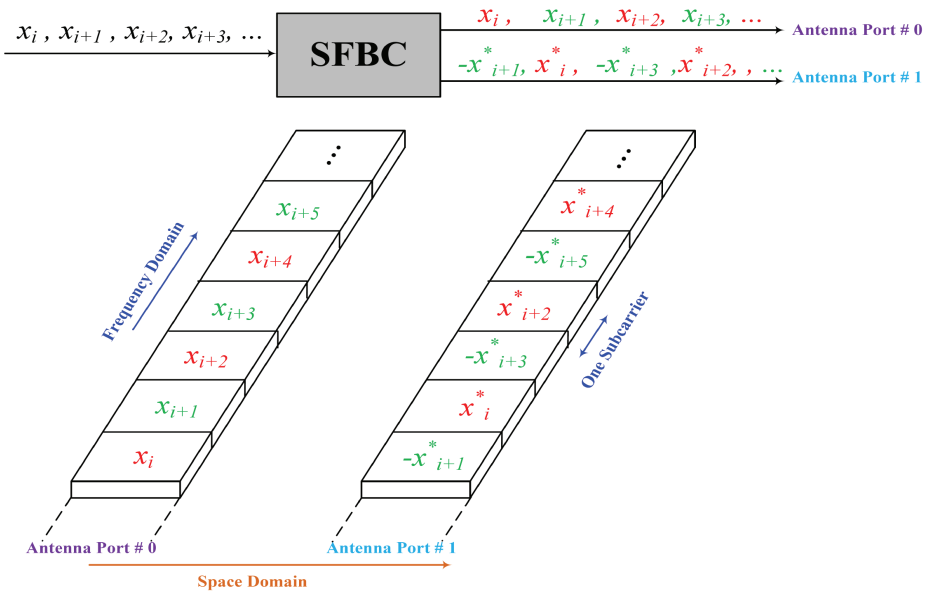

Fig. 3. Space Frequency Block Coding (SFBC) Scheme in LTE [11].

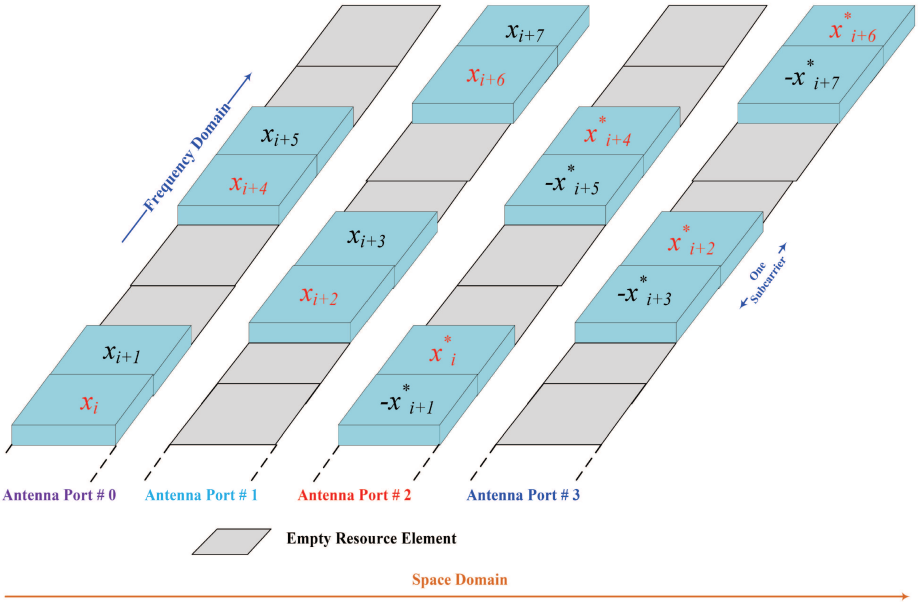

Fig. 4. Frequency Switched Transmit Diversity (FSTD) Scheme in LTE [11].

C. Transmit Diversity Schemes in LTE

In LTE, two main transmit diversity schemes are employed; the first one (SFBC scheme) with 2 transmit antennas and the second one (FSTD scheme) with 4 transmit antennas [10]. Both schemes use only one data stream (one signal) [11]. In LTE, one data signal (also called data stream) is referred as one codeword because only one transport block (TB) is used per data stream. In order to ensure uncorrelated channels between different antennas and hence maximizing the diversity gain, the antennas should be well separated relative to the wavelength.

1) SFBC scheme in LTE: When a physical channel in LTE is configured for transmit diversity operation using two eNodeB antennas, the diversity scheme is called Space Frequency Block Coding. The principle of SFBC transmission is shown in Figure 3, similarly to the one reported in [11]. As can be seen from Figure 3, the SFBC diversity scheme is, in fact, the frequency domain implementation of the well known Space Time Block Coding technique, developed by Alamouti [12]. The fundamental characteristic of this family of coding is that the transmitted diversity streams are orthogonal and they can be simply decoded at the receiver.

STBC operates on pairs of adjacent symbols in the time domain. Since the signal in LTE is two dimensional (time and frequency domains) and the number of available OFDM symbols in a subframe is not always an even number, the direct application of STBC is not straightforward. Therefore, SFBC scheme is proposed to be employed.

In LTE, for SFBC transmission, the symbols are transmitted from two eNodeB antenna ports on each pair of adjacent subcarriers as follows [10]:

$$\begin{bmatrix} y^{(0)}(2j) & y^{(0)}(2j+1) \\ y^{(1)}(2j) & y^{(1)}(2j+1) \end{bmatrix} = \begin{bmatrix} x_{2j} & x_{2j+1} \\ -x^*_{2j+1} & x^*_{2j} \end{bmatrix} \quad (4)$$

where $y^{(p)}(k)$ denotes the symbols transmitted on the k-th subcarrier from antenna port p. x_{2j} and x_{2j+1} ($j = 0, 1, 2, ..., \frac{N}{2} - 1$) are two adjacent subcarriers in the OFDM modulated signals, explained earlier. An important characteristic of such codes is that the transmitted signal streams are orthogonal and a simple linear receiver can be used for detection and decoding of the signal.

2) FSTD scheme in LTE: The diversity scheme in case of four transmit antennas (operating on port 0 to port 3) is called Switched Transmit Diversity [10]. The transmission structure for FSTD diversity scheme is shown in Figure 4, similarly to the one explained in [11]. In the FSTD scheme a pair of modulated symbols are transmitted using SFBC scheme over two antennas, whereas the other two antennas are not transmitting. In other words, in the FSTD scheme, the transmission is switched between a pair of transmit antennas at each frequency slot. This means that in the first frequency slot the first two symbols are transmitted through antenna port 0 and antenna port 2, whereas nothing is transmitted on antennas ports 1 and 3. Then, in the next frequency slot for transmission of next two symbols, antenna ports 1 and 3 are used, where antenna ports 0 and 2 are not transmitting. In LTE, the space frequency block code, designed for FSTD employing 4 transmit antennas is defined as follows:

$$\begin{bmatrix} y^{(0)}(4j) & y^{(0)}(4j+1) & y^{(0)}(4j+2) & y^{(0)}(4j+3) \\ y^{(1)}(4j) & y^{(1)}(4j+1) & y^{(1)}(4j+2) & y^{(1)}(4j+3) \\ y^{(2)}(4j) & y^{(2)}(4j+1) & y^{(2)}(4j+2) & y^{(2)}(4j+3) \\ y^{(3)}(4j) & y^{(3)}(4j+1) & y^{(3)}(4j+2) & y^{(3)}(4j+3) \end{bmatrix} =$$

$$\begin{bmatrix} x_{4j} & x_{4j+1} & 0 & 0 \\ 0 & 0 & x_{4j+2} & x_{4j+3} \\ -x^*_{4j+1} & x^*_{4j} & 0 & 0 \\ 0 & 0 & -x^*_{4j+3} & x^*_{4j+2} \end{bmatrix} \quad (5)$$

where $y^{(p)}(k)$ denotes the symbols transmitted on the k-th subcarrier from antenna port p. x_{4j}, x_{4j+1}, x_{4j+2}, and x_{4j+3}, ($j = 0, 1, 2, ..., \frac{N}{4} - 1$) are 4 adjacent subcarriers in the OFDM modulated signals, explained earlier.

In the following, we present a performance analysis and evaluation for three important metrics, namely the average BER, the average capacity, and the average throughput of the considered MIMO systems in LTE.

III. Performance Analysis

In the following, we first present a performance analysis for the average BER of 2×1 MIMO SFBC and 4×2 MIMO FSTD systems, over slow fading channels. Then an analysis for the channel capacity of the considered systems is presented, followed by the average throughput evaluation. The channel capacity and throughput results can be considered as a performance limit in terms of bits/sec/Hz for the LTE system. Finally, the numerical results, obtained from closed-form expressions as well as the results obtained from Monte-carlo simulations, are presented to verify the accuracy of our analysis.

A. Average BER Performance Analysis

In the following, we present the average BER analysis for the SFBC and SFTD systems. For each case, we first briefly describe the transmit diversity and space frequency coding scheme. Then, using the Moment Generating Function (MGF)-based approach, closed-form expressions are obtained for the average BER performance of the system for 2×1 SFBC and 4×2 FSTD MIMO schemes.

1) BER Analysis of SFBC: As explained earlier for Figure 3, SFBC-OFDM transmit diversity scheme is in fact a 2×1 MIMO system employing space frequency block coding over N OFDM subcarriers.

Since OFDM converts the multipath fading channel into N frequency flat fading sub-channels, we first derive the BER expressions over flat Rayleigh fading sub-channels, given by $P_b(E)$. Then, the overall average BER over N sub-channels, in each case can be calculated from

$$BER_{avg} = \frac{1}{N} \sum_{k=1}^{N} P_{b,k}(E) \quad (6)$$

where the index k (subcarrier/sub-channel index) is ignored for the sake of brevity. In addition, the impact of cyclic prefix in OFDM is assumed to be negligible.

For the 2×1 MIMO system employing SFBC scheme, the probability density function of the SNR for each subcarrier is given by a chi-square distribution function as follows [13]

$$f_\gamma(\gamma) = \frac{2}{\bar{\gamma}^2} \gamma e^{-\frac{2}{\bar{\gamma}}\gamma} \quad (7)$$

where $\bar{\gamma}$ is the average SNR per symbol given by $\bar{\gamma} = E_s/N_0$.

The moment generating function (MGF) can be determined using the following equation:

$$M_{\bar{\gamma}}(s) = \int_0^\infty e^{-s\gamma} f(\gamma) d\gamma. \quad (8)$$

Inserting (7) into (8) and solving the integral yields

$$M_{\bar{\gamma}}(s) = \frac{4}{\bar{\gamma}^2 (s + \frac{2}{\bar{\gamma}})^2}. \quad (9)$$

The average BER expression for M-QAM modulation scheme can be obtained from [14] (equation (8.111; Page 255))

$$P_b(E) \cong B \sum_{i=1}^{\sqrt{M}/2} \frac{1}{\pi} \int_0^{\pi/2} M_{\bar{\gamma}}(A_{i,\theta})\, d\theta \quad (10)$$

where $A_{i,\theta} = \frac{(2i-1)^2}{2\sin^2\theta}\frac{3}{(M-1)}$ and B is defined by

$$B = 4\left(\frac{\sqrt{M}-1}{\sqrt{M}}\right)\left(\frac{1}{\log_2 M}\right). \quad (11)$$

Then, using the MGF expression in (9), we obtain

$$M_{\bar{\gamma}}(A_{i,\theta}) = \frac{4}{\bar{\gamma}^2\left(\left[\frac{(2i-1)^2}{2\sin^2\theta}\frac{3}{(M-1)}\right]+\frac{2}{\bar{\gamma}}\right)^2}. \quad (12)$$

Substituting (12) into (10) and after some manipulations, we obtain

$$P_b(E) \cong B\sum_{i=1}^{\sqrt{M}/2}\frac{1}{\pi}\int_0^{\pi/2}\left(\frac{\sin^2\theta}{\sin^2\theta + c_i}\right)^2 d\theta \quad (13)$$

where $c_i = \frac{3(2i-1)^2}{2(M-1)}\frac{\bar{\gamma}}{2}$.

The average BER performance as a function of $\bar{\gamma} = E_s/N_0$ can be evaluated by numerical evaluation of the integral in (13) for M-QAM modulation schemes.

Alternatively, by solving the integral, we obtain a closed-form expression for the average BER of M-QAM modulation as follows

$$P_b(E) \cong B\sum_{i=1}^{\sqrt{M}/2}\mathcal{I}_2(\pi/2, c_i) \quad (14)$$

where the closed-form expression for $\mathcal{I}_2(.,.)$ can be obtained from [14](eq.5A.24) as follows

$$\mathcal{I}_n(\phi, D) = \frac{1}{\pi}\int_0^{\phi}\left(\frac{\sin^2\theta}{\sin^2\theta + D}\right)^n d\theta, \qquad -\pi \le \phi \le \pi \quad (15)$$

$$= \frac{\phi}{\pi} - \frac{\beta}{\pi}\left\{\left(\frac{\pi}{2} + \tan^{-1}\alpha\right)\sum_{q=0}^{n-1}\binom{2q}{q}\frac{1}{(4(1+D))^q} + \sin\left(\tan^{-1}\alpha\right)\sum_{q=1}^{n-1}\sum_{p=1}^{q}\frac{T_{p\,q}}{(1+D)^q}\left[\cos\left(\tan^{-1}\alpha\right)\right]^{2(q-p)+1}\right\} \quad (16)$$

where $T_{p\,q} = \binom{2q}{q}\left[\binom{2(q-p)}{q-p}4^p\left[2(q-p)+1\right]\right]^{-1}$, $\beta = \sqrt{\frac{D}{1+D}}\,\mathrm{sgn}\phi$, and $\alpha = -\beta\cot\phi$.

2) BER Analysis of FSTD: As discussed earlier for Figure 4, FSTD-OFDM transmit diversity scheme is a 4×2 MIMO system employing space frequency block coding over N OFDM subcarriers, in which only 2 transmit antennas out of 4 antennas are used at each transmission slot. In this case, considering two consecutive slots, in the first slot only antenna ports 0 and 2 are used for transmissions and in the second slot only antenna ports 1 and 3 are employed for transmissions.

For the 4×2 MIMO system employing FSTD-OFDM scheme, we can show that the instantaneous SNR of the system, for k-th subcarrier, is equivalent to that for a 2×2 STBC MIMO system. Therefore, the probability density function of the SNR is given by a chi-square distribution function as follows [13]

$$f_\gamma(\gamma) = \frac{8}{3\bar{\gamma}^4}\gamma^3 e^{-\frac{2}{\bar{\gamma}}\gamma}. \quad (17)$$

In this case, the MGF expression can be obtained by substituting (17) into (8), which yields

$$M_{\bar{\gamma}}(s) = \frac{16}{\bar{\gamma}^4(s+\frac{2}{\bar{\gamma}})^4}. \quad (18)$$

Similarly to the SFBC case discussed earlier, inserting (18) into (10), the average BER expression with M-QAM modulation for FSTD can be written as

$$P_b(E) \cong B\sum_{i=1}^{\sqrt{M}/2}\frac{1}{\pi}\int_0^{\pi/2}\left(\frac{\sin^2\theta}{\sin^2\theta + c_i}\right)^4 d\theta \quad (19)$$

where $c_i = \frac{3(2i-1)^2}{2(M-1)}\frac{\bar{\gamma}}{2}$, and the integral can be calculated numerically.

Alternatively, by solving the integral, we obtain a closed-form expression for the average BER of M-QAM modulation for FTSD as follows

$$P_b(E) \cong B\sum_{i=1}^{\sqrt{M}/2}\mathcal{I}_4(\pi/2, c_i) \quad (20)$$

where the closed-form expression for $\mathcal{I}_4(.,.)$ can be obtained from (16).

Finally, for the sake of comparisons, we express the average BER of the single-input single-output (SISO) system, that has been derived for Rayleigh fading channels for M-QAM signals [14] (eq. 8.112; Page 256), as follows:

$$P_b(E) \cong B/2\sum_{i=1}^{\sqrt{M}/2}\left(1 - \sqrt{\frac{1.5(2i-1)^2\overline{\gamma}\log_2 M}{M - 1 + 1.5(2i-1)^2\overline{\gamma}\log_2 M}}\right) \quad (21)$$

where B is defined earlier.

B. Average Channel Capacity Analysis

The channel capacity of the MIMO-OFDM system employing a space-frequency code for the k-th subcarrier at n-th time instant can be written as [15], [16]:

$$C_{k,n} = R_c\,\log_2\left(1 + \frac{\overline{\gamma}}{N_{\mathrm{T}}R_c}\|\mathbf{H}_{k,n}\|_F^2\right). \quad (22)$$

It can be also expressed as

$$C_{k,n} = R_c\,\log_2(1 + \gamma_{k,n}) \quad (23)$$

where $\gamma_{k,n} = \frac{\overline{\gamma}}{N_T R_c} \|\mathbf{H}_{k,n}\|_F^2$ and R_c is the SFBC code rate, that is equal to one ($R_c = 1$) for Alamouti space-time coding used in SFBC and FSTD schemes.

The average capacity averaged over time instant n for k subcarrier can be written as

$$\overline{C}_k = E\{C_{k,n}\} = \int_0^\infty R_c \log_2(1+\gamma_{k,n})\, f_{\gamma_{k,n}}(\gamma_{k,n})\, d\gamma_{k,n}. \quad (24)$$

Finally, by averaging over N subchannels, the overall average channel capacity can be obtained from

$$\mathrm{C}_{\mathrm{avg}} = \frac{1}{N} \sum_{k=0}^{N-1} \overline{C}_k. \quad (25)$$

1) Channel Capacity of SFBC MIMO-OFDM: For the 2×1 SFBC MIMO-OFDM scheme, the probability density function of the SNR for each subcarrier is given by (7). Inserting (7) into (24), we obtain

$$\begin{aligned}\overline{C}_k &= \int_0^\infty R_c \log_2(1+\gamma)\, \frac{2}{\bar{\gamma}^2} \gamma e^{-\frac{2}{\bar{\gamma}}\gamma}\, d\gamma \\ &= R_c \log_2(e) \int_0^\infty \frac{2}{\bar{\gamma}^2} \ln(1+\gamma)\, \gamma e^{-\frac{2}{\bar{\gamma}}\gamma}\, d\gamma. \end{aligned} \quad (26)$$

To solve the above integral, we use the following result [17]

$$\begin{aligned}&\frac{\mu}{(M-1)!} \int_0^\infty \ln(1+x)\, (\mu x)^{M-1}\, e^{-\mu x}\, dx \\ &= \mathcal{P}_M(-\mu)\, E_1(\mu) + \sum_{j=1}^{M-1} \frac{1}{j}\, \mathcal{P}_j(\mu)\, \mathcal{P}_{M-j}(-\mu) \end{aligned} \quad (27)$$

where $\mathcal{P}_M(.)$ is the Poisson distribution defined by $\mathcal{P}_M(x) = \sum_{v=0}^{M-1} \frac{x^v}{v!} e^{-x}$, and where $E_1(.)$ is the exponential integral of first order, defined by $E_1(x) = \int_x^\infty t^{-1} e^{-t} dt$ for $x > 0$.

Therefore, using (27) and after performing changes of variables together with some simplifications, we obtain the solution of integral in (26) as

$$\overline{C}_k = A_1 \left[\mathcal{P}_1(-\mu)\, E_1(\mu) + \mathcal{P}_1(\mu)\, \mathcal{P}_1(-\mu)\right] \quad (28)$$

where $A_1 = R_c \log_2(e)$ and $\mu = \frac{2}{\bar{\gamma}}$. Then the overall average channel capacity can be obtained from (25).

2) Channel Capacity of FSTD MIMO-OFDM: As mentioned earlier, for the 4×2 FSTD MIMO-OFDM scheme, we can show that the instantaneous SNR of the system, for k-th subcarrier, is equivalent to that for a 2×2 SFBC MIMO-OFDM scheme. For the 2×2 SFBC MIMO-OFDM scheme, the probability density function of the SNR for each subcarrier is given by (17).

Similar to the 2×1 SFBC MIMO-OFDM case, substituting (17) into (24), we can obtain

$$\overline{C}_k = A_2 \left[\mathcal{P}_4(-\mu)\, E_1(\mu) + \sum_{j=1}^{3} \frac{1}{j}\, \mathcal{P}_j(\mu)\, \mathcal{P}_{4-j}(-\mu)\right] \quad (29)$$

where $A = R_c \log_2(e)/3$ and $\mu = \frac{2}{\bar{\gamma}}$. Then the overall average channel capacity can be obtained from (25).

C. Throughput Analysis

In a frequency selective fading channel, the subchannels corresponding the OFDM subcarriers have different amplitudes. To obtain a better throughput or a spectral efficiency, the transmission mode on each subcarrier can be chosen according the subchannels state information. Using the known channel state information (CSI), the transmitter can choose the best modulation mode and can adapt the transmission rate and/or transmit power on each OFDM subcarrier. Here, we consider an adaptive modulation with constant-power and adaptive-rate transmission while satisfying a quality of service (QoS) indicator such as a predefined target BER or a target Block error rate (BLER). We use a rate adaptive modulation assuming L-mode square M-QAM modulations.

To perform adaptive modulation we divide the entire SNR region into $L+1$ fading regions. Then, according the instantaneous SNR value on each subchannel in each SNR region, we assign the best modulation mode. This method can provide the largest throughput while satisfying a target BER value [15].

In this case, the throughput (in Bits/Sec/Hz) for the considered MIMO-OFDM systems is defined as [15], [16], [18]:

$$T_{avg} = \frac{R_c}{N} \sum_{k=0}^{N-1} \sum_{l=1}^{L} \beta_l[k] \left[F_\gamma(\alpha_{l+1}) - F_\gamma(\alpha_l)\right] \quad (30)$$

where $\beta_l[k]$ is the number of bits assigned in l-th SNR region for k-th OFDM subcarrier, α_l and α_{l+1} are the switching SNR thresholds for l-th SNR region. $F_\gamma(\gamma)$ is the cumulative distribution function (CDF) defined as $F_\gamma(\alpha_j) = \int_{-\infty}^{\alpha_j} f_\gamma(\gamma)\, d\gamma$, where $f_\gamma(\gamma)$ is defined earlier for each MIMO-OFDM scheme. We can simply show that substituting the $f_\gamma(\gamma)$ expressions for 2×1 SFBC MIMO-OFDM and 4×2 FSTD MIMO-OFDM respectively given by (7) and (17) in it we obtain

$$F_\gamma(\gamma) = 1 - e^{-\frac{2}{\bar{\gamma}}\gamma} \left(1 + \frac{2}{\bar{\gamma}}\right) \quad (31)$$

and

$$F_\gamma(\gamma) = 1 - e^{-\frac{2}{\bar{\gamma}}\gamma} \left(1 + \frac{2}{\bar{\gamma}} + \frac{2}{\bar{\gamma}^2} + \frac{8}{3\bar{\gamma}^3}\right). \quad (32)$$

Finally, closed-form expressions for the average throughput of 2×1 SFBC MIMO-OFDM and 4×2 FSTD MIMO-OFDM systems can be obtained by inserting the corresponding CDF expressions (31) and (32) into (30), respectively.

TABLE I
SIMULATION SETTINGS

Parameter	Setting
Transmission Schemes	SISO; 2×1 SFBC; 4×2 FSTD
Bandwidth	5 MHz
Simulation length	5000 subframes
Channel Type	Rayleigh Fading
Channel knowledge	Perfect
CQI	6 (QPSK), 9 (16-QAM), and 16 (64-QAM)

IV. SIMULATION AND ANALYTICAL RESULTS

In this section, we provide the performance results obtained from the mathematical expressions derived in this paper for the average BER, the average capacity and the average throughput of the considered MIMO systems in LTE, and assuming $\overline{\gamma} = E_s/N_0$ and $R_c = 1$. Monte-Carlo simulation results are also provided to show the accuracy of the analysis.

The common simulation settings for Monte-Carlo simulations are summarized in Table I.

A. Average BER Performance results

The average BER performance as a function of $\overline{\gamma} = Es/N_0$ for SISO and MIMO schemes are shown in Figure 5, Figure 6, and Figure 7. In Figure 5, the average BER results are provided assuming 4-QAM, i.e., QPSK modulation. Figure 6 shows the results for 16-QAM modulation and Figure 7 presents the results for 64-QAM modulation.

It can be seen that the average BER performances of QPSK, 16-QAM, and 64-QAM schemes at high SNRs decrease by factors $\overline{\gamma}^1$, $\overline{\gamma}^2$, and $\overline{\gamma}^4$, for SISO, 2×1, and 4×2 MIMO cases, respectively. Thus, the diversity order (slope of the curves) are equal to 1, 2 and 4, respectively, for the considered cases. As stated earlier, since in 4×2 FSTD, at each time-slot/frequency-slot 2 out of 4 transmit antennas are in use, therefore the diversity order will be $2 \times 2 = 4$. In fact, the corresponding average BER curve for 4×2 FSTD is somehow like the classical 2×2 STBC system, when the channel is not a time-varying channel.

From the figures it is clear that the BER performance improves as the number of transmit or receive antennas increases, as expected. It can be observed that the negative slope of the BER curve for the SISO case is equal to 1, meaning that the diversity order for the SISO case is equal to 1, as expected.

The second curves in Figure 5, Figure 6, and Figure 7 represent the BER results of the 2×1 SFBC diversity scheme. Asymptotically, the slope of these curves can be observed to be equal to 2, which corresponds to the diversity order of 2×1 SFBC system. An SNR (Es/N_0) gain improvement can also be observed compared to the SISO scheme. From Figure 6, it can be observed that to achieve the BER value of 10^{-3}, the 2×1 diversity scheme needs about 10 dB less in Es/N_0, compared to the SISO case.

In Figure 7 for 64-QAM modulation, the average BER of 10^{-3} is achieved at $Es/N_0 = 39$ dB in SISO configuration, however, the same value of BER is achieved with only at $Es/N_0 = 29$ dB in the 2×1 diversity scheme. Thus an SNR gain of 10 dB is clearly observed for the 2×1 diversity

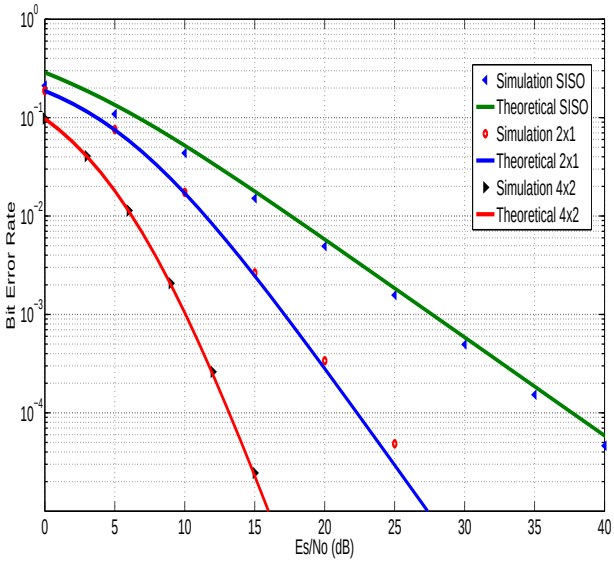

Fig. 5. Numerical Evaluation and Monte-Carlo Simulations of the average BER for QPSK modulation.

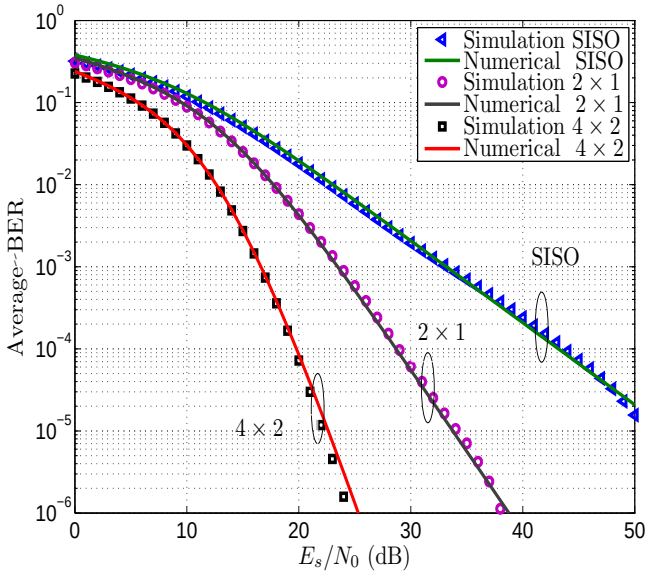

Fig. 6. Numerical Evaluation and Monte-Carlo Simulations of the average BER for 16-QAM modulation.

scheme. The BER results of the 4×2 diversity scheme for both modulation schemes, i.e., 16-QAM and 64-QAM are also shown. As described earlier, in high SNRs region the slope of that curve tends to be equal to 4. This value corresponds to the diversity order of a 2×2 system.

Finally, it can be observed from Figure 5, Figure 6 and Figure 7 that numerical evaluation results obtained from average BER formulas match closely to the average BER results obtained from Monte-Carlo simulations. This verifies the accuracy of the analysis.

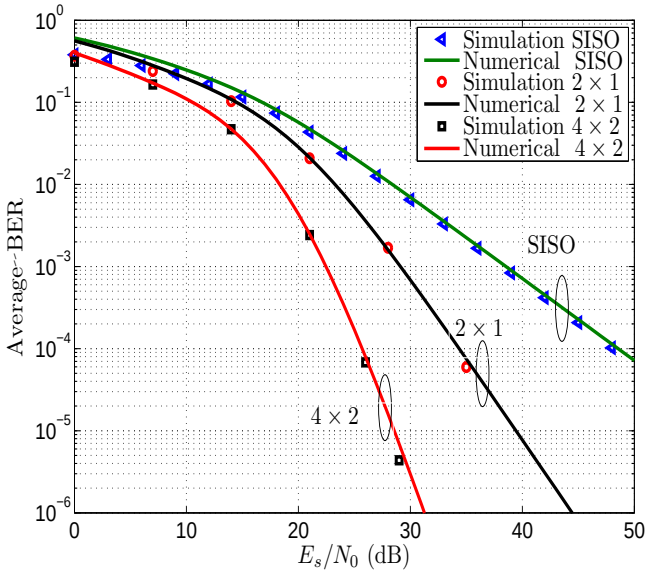

Fig. 7. Numerical Evaluation and Monte-Carlo Simulations of the average BER for 64-QAM modulation.

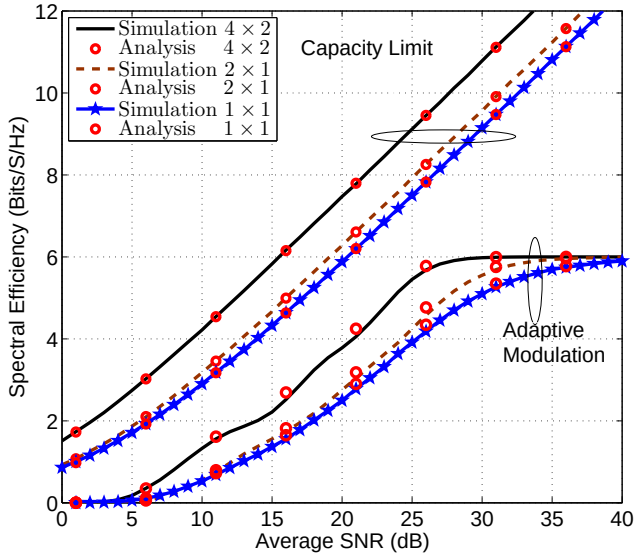

Fig. 9. Numerical Evaluation and Monte-Carlo Simulations of the average spectral efficiency of the system for different cases.

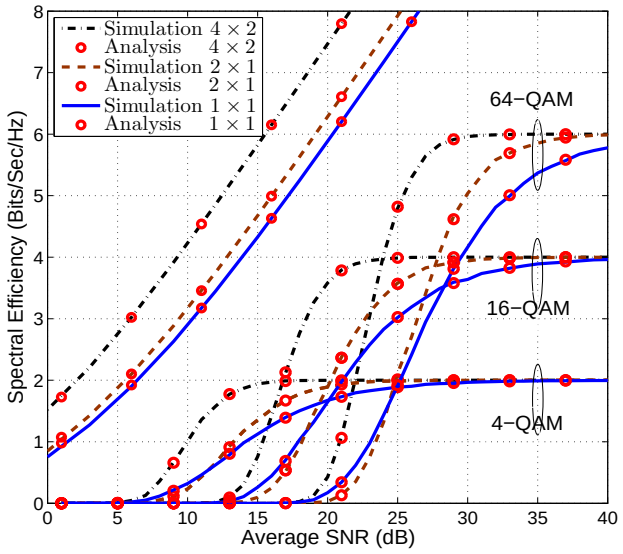

Fig. 8. Numerical Evaluation and Monte-Carlo Simulations of the average spectral efficiency of the system for different cases.

B. Average Channel Capacity and Throughput Results

In the following, we show the results for the average capacity and the average throughput (average spectral efficiency) results for the considered systems. The results are obtained from the mathematical formulas presented in previous section as well as from Monte-Carlo simulations. Figure 8 and Figure 9 show the channel capacity limits as well as the throughput of 2×1 SFBC MIMO-OFDM, 4×2 FSTD MIMO-OFDM, and SISO-OFDM systems. For evaluating the throughout, we assume several cases considering a target BER of 10^{-5}.

In Figure 8, we assume a case using two transmission modes, i.e., one M-QAM transmission mode ($M \in \{4, 16, 64\}$) and a no-transmission mode. For example, when 16-QAM modulation and no-transmission modes are considered, when the SNR of the subchannel is below a certain threshold we use 16-QAM for transmission, otherwise no data is transmitted, i.e., no-transmission mode. The SNR threshold is obtained according the target BER value. It can be observed in Figure 8 that the capacity for 4×2 FSTD MIMO-OFDM system is superior than those of 2×1 SFBC MIMO-OFDM, and SISO cases, as expected.

It is also shown that 2×1 SFBC MIMO-OFDM system can provide superior capacity performance compared to the SISO system. It can be observed that in a two-mode transmission case, using a higher modulation mode (e.g., 16-QAM instead of 4-QAM) yields a throughput increase at high SNRs. However, at low SNR values, for example between 8 to 20 dB, 4-QAM transmission can provide a higher throughput than 64-QAM case. This is due to the fact that the SNR threshold for 4-QAM is much less than that for 64-QAM, and a two-mode transmission using 4-QAM starts the transmission at a lower SNR than for a two-mode transmission using 64-QAM.

To obtain a better throughput, we use more modulation modes in the transmission. In Figure 9, we assume a case using several transmission modes, including a no-transmission mode, and a four-transmission mode using BPSK, 4-QAM, 16-QAM, 64-QAM schemes. In this case, we obtain 4 SNR thresholds α_l ($l = 1, 2, 3, 4$) corresponding to the considered modulation schemes and satisfying the target BER of 10^{-5}. It can be seen that transmissions occur in a wide range of SNR values. In 1×1 SISO system, and in 2×1, and 2×4 MIMO systems, the throughput values reach a maximum rate of 6 bits/sec/Hz that is equal to the average bits transmitted by 64-QAM, the highest mode considered. To verify the analysis the results obtained from Monte-carlo simulations are also provided. It can be seen that the numerical results obtained from the formulas match closely to the simulation results.

V. Conclusion

In this paper, we have presented performance analyses for the average BER, the average channel capacity and the throughput of MIMO schemes in the 3GPP Long Term Evolution (LTE). The theoretical analysis for two different MIMO schemes in a 5 MHz bandwidth LTE system were presented. To verify the accuracy of the analysis the results of Monte-Carlo simulation for the studied schemes were provided and compared with the results obtained from theoretical analysis. To show the performance improvement in the MIMO schemes, the performance of a SISO configuration was also presented. The results show a good agreement between numerical results and Monte-Carlo simulation results.

References

[1] A. Jemmali, J. Conan, and M. Torabi, "Bit Error Rate Analysis of MIMO Schemes in LTE Systems," in *Proc. International Conference on Wireless and Mobile Communications (ICWMC-2013)*, July 2013, pp. 190–194.

[2] C. Mehlführer, M. Wrulich, J. C. Ikuno, D. Bosanska, and M. Rupp, "Simulating the long term evolution physical layer," in *Proc. European Signal Processing Conference (EUSIPCO 2009)*, 2009.

[3] Online, "LTE link level simulator," 2009, available http://www.nt.tuwien.ac.at/ltesimulator.

[4] J. Ikuno, M. Wrulich, and M. Rupp, "System level simulation of LTE networks," in *Proc. IEEE Vehicular Technology Conference (VTC 2010-Spring)*, May 2010, pp. 1–5.

[5] M. Simko, C. Mehlfuhrer, M. Wrulich, and M. Rupp, "Doubly dispersive channel estimation with scalable complexity," in *Proc. International ITG Workshop on Smart Antennas (WSA)*, Feb. 2010, pp. 251–256.

[6] S. Schwarz, M. Wrulich, and M. Rupp, "Mutual information based calculation of the precoding matrix indicator for 3GPP UMTS/LTE," in *2010 International ITG Workshop on Smart Antennas (WSA)*, Feb. 2010, pp. 52–58.

[7] S. Schwarz, C. Mehlfuhrer, and M. Rupp, "Calculation of the spatial preprocessing and link adaption feedback for 3GPP UMTS/LTE," in *Proc. 6th Conference on Wireless Advanced (WiAD)*, June 2010, pp. 1–6.

[8] A. Jemmali, *Performance Evaluation and Analysis of MIMO Schemes in LTE Networks Environment*. PhD Thesis, Université De Montréal, École Polytechnique De Montréal, Quebec, Canada., 2013.

[9] D. Tse and P. Viswanath, *Fundamnetals of Wireless Communications*. Cambridge University Press, 2008.

[10] S. Sesia, T. Issam, and M. Backer, *LTE The UMTS Long Term Evolution From Theory To Practice*. John Wiley, 2011.

[11] E. Dahlman, S. Parkvall, and J. Skld, *4G LTE/LTE-Advanced for Mobile Broadband*. Academic Press, Elsevier, 2011.

[12] S. Alamouti, "A simple transmit diversity technique for wireless communications," *IEEE Journal on Selected Areas in Communications*, vol. 16, no. 8, pp. 1451–1458, Oct. 1998.

[13] M. Torabi and D. Haccoun, "Performance Analysis of Joint User Scheduling and Antenna Selection Over MIMO Fading Channels," *IEEE Signal Process. Lett.*, vol. 18, no. 4, pp. 235–238, April 2011.

[14] M. S. Alouini and M. K. Simon, *Digital Communications over Fading Channels: A Unified Approach to Performance Analysis*. Wiley, 2000.

[15] M. Torabi, D. Haccoun, and W. Ajib, "Performance Analysis of Scheduling Schemes for Rate-Adaptive MIMO OSFBC-OFDM Systems," *IEEE Trans. Veh. Technol.*, vol. 59, no. 5, pp. 2363–2379, June 2010.

[16] L. Hanzo, C. H. Wong, and M. S. Yee, *Adaptive wireless transceivers: Turbo-Coded, Turbo-Equalised and Space-Time Coded TDMA, CDMA and OFDM Systems*. John Wiley & Sons Ltd, 2002.

[17] C. G. Günther, "Comment on estimate of channel capacity in Rayleigh fading environment," *IEEE Trans. Veh. Technol.*, vol. 45, no. 2, pp. 401–403, May 1996.

[18] M. S. Alouini and A. J. Goldsmith, "Adaptive modulation over Nakagami fading channels," *Wireless Personal Communications*, vol. 13, no. 1, pp. 119–143, 2000.